

3.3 General Fluid Formulation

We have used conservation laws to study flow through a 1-D control volume to analyze normal shocks. To study more general flows around hypersonic vehicles we must include additional phenomena:

- ▶ unsteady, multi-dimensional flow
- ▶ mixture of chemical species
- ▶ real gas effects
- ▶ molecular transport processes
- ▶ turbulence

Today, we present a general fluid formulation that allows study of these effects.

3.2 Navier-Stokes Equations

Named after Claude-Louis Navier and George Gabriel Stokes

The Navier-Stokes equations technically only references the momentum conservation equations expressed with viscous effects

However, the term is generally used to described the set of conservation equations (mass, momentum, energy) necessary to described a viscous flow

The equation can derived using the usual conservation laws

3.2 Navier-Stokes Equations

a) Mass

Conservation of mass for chemical species s is:

$$\frac{\partial \rho_s}{\partial t} + \nabla \cdot (c_s \rho \mathbf{v}) - \nabla \cdot (\rho \boldsymbol{\Gamma}_s) = \dot{w}_s \quad (3.26)$$

where

- ▶ c_s = mass fraction of s : $c_s = \frac{\rho_s}{\rho} = \frac{\rho_s}{\sum_s \rho_s}$
- ▶ \mathbf{v} = mass-averaged velocity
- ▶ $\nabla \cdot (\rho \boldsymbol{\Gamma}_s)$ = mass flux due to diffusion
- ▶ \dot{w}_s = source term due to chemistry
- ▶ $\boldsymbol{\Gamma}_s = c_s(\mathbf{v} - \mathbf{v}_s)$

Summation of Eq. (3.26) over all chemical species gives:

$$\frac{\partial \rho}{\partial t} + \nabla \cdot (\rho \mathbf{v}) = 0 \quad (3.27)$$

Note: for reacting flows, mass conservation equation, Eq. (3.26), is needed for each species

3.2 Navier-Stokes Equations

b) Momentum

Neglecting body forces, including pressure and shear stress forces

$$\rho \left(\frac{\partial \mathbf{v}}{\partial t} + (\mathbf{v} \cdot \nabla) \mathbf{v} \right) = -\nabla p + \nabla \cdot \boldsymbol{\tau} \quad (3.28)$$

where

- ▶ $\boldsymbol{\tau}$ = shear stress tensor

Here, the conservation equation is unaffected by air chemistry (although, $\boldsymbol{\tau}$ is affected)

3.2 Navier-Stokes Equations

c) Energy

Using total specific energy $e_t \equiv e + \frac{1}{2}v^2$:

$$\frac{\partial}{\partial t} \rho e_t + \nabla \cdot (\rho \mathbf{v} e_t) + \nabla \cdot (p \mathbf{v}) - \nabla \cdot (\boldsymbol{\tau} \cdot \mathbf{v}) + \nabla \cdot \mathbf{q} - \nabla \cdot \left(\sum_s h_s \rho \boldsymbol{\Gamma}_s \right) = 0$$

where:

(3.29)

- ▶ (1) : rate of change of total energy per unit volume
- ▶ (2) : flux of total energy
- ▶ (3) : rate of work due to pressure forces
- ▶ (4) : rate of work done by shear stress forces due to velocity gradients
- ▶ (5) : thermal conduction due to temperature gradients
- ▶ (6) : diffusion of enthalpy due to concentration gradients

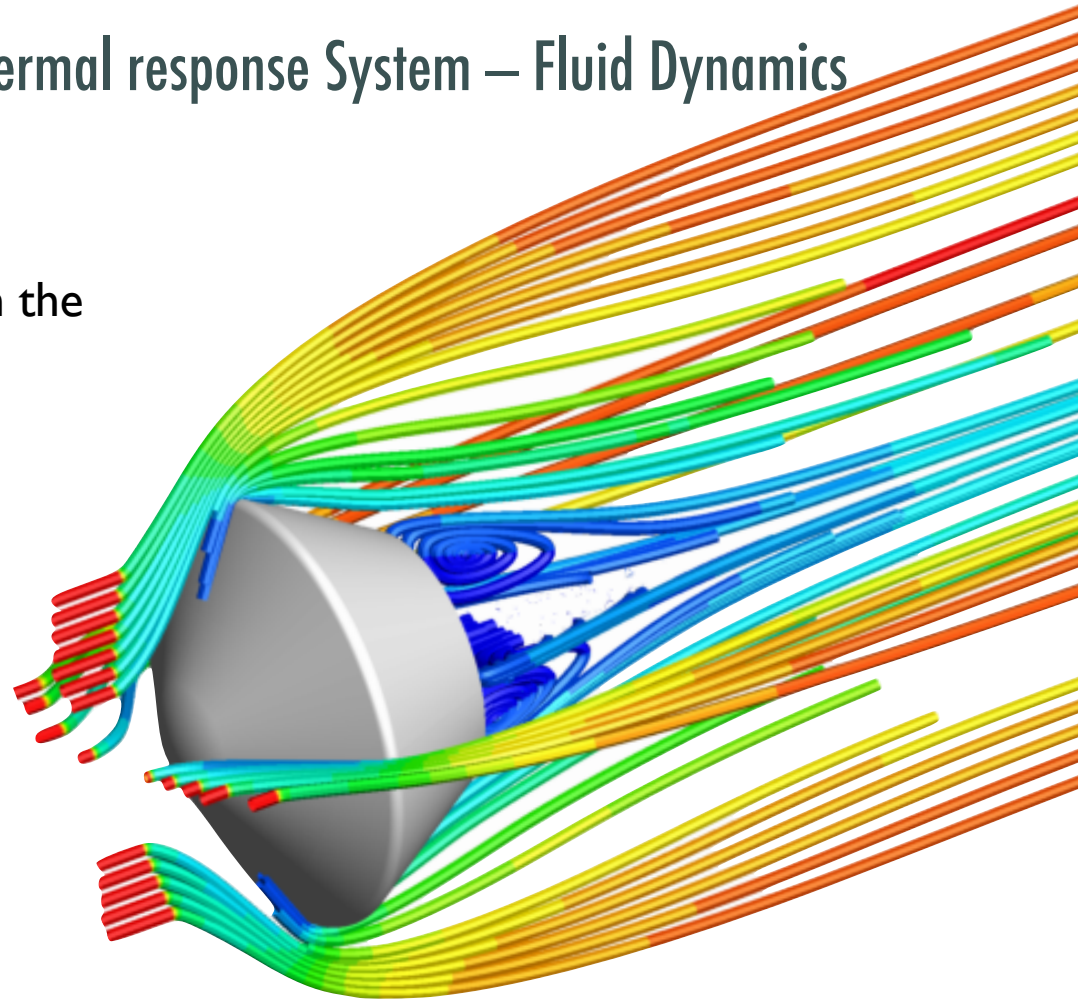
Terms (4) to (6) involve molecular transport processes

Analytical solution of these equations is impossible for general situations. Instead, we use Computational Fluid Dynamics (CFD)

KATS-FD

Kentucky Aerothermodynamics and Thermal response System – Fluid Dynamics

- Developed at the University of Kentucky in the Gas-Surface Interaction Lab
- A multi-dimensional, parallel CFD code for the simulation of weakly ionized hypersonic flows in thermo-chemical non-equilibrium
- Solves the Navier-Stokes equations modified to include finite-rate chemistry and relaxation rates to compute the different energy modes (2 temperatures)
- Solves the equations over a mixed unstructured grid
- Calculates the inviscid fluxes using a modified form of the Steger-Warming Flux Vector Splitting scheme



Stardust flow field (Zhang, 2012)



KATS — Modeling Framework

- [1] Weng, H. and Martin, A., "Multidimensional modeling of pyrolysis gas transport inside charring ablative materials," Journal of Thermophysics and Heat Transfer, Vol. 28, No. 4, October–December 2014, pp. 583–597.
- [2] Weng, H., Bailey, S. C. C., and Martin, A., "Numerical study of iso-Q sample geometric effects on charring ablative materials," International Journal of Heat and Mass Transfer, Vol. 80, January 2015, pp. 570–596.
- [3] Weng, H. and Martin, A., "Numerical Investigation of Thermal Response Using Orthotropic Charring Ablative Material," Journal of Thermophysics and Heat Transfer, Vol. 29, No. 3, July 2015, pp. 429–438.
- [4] Davuluri, R. S. C., Zhang, H., and Martin, A., "Numerical study of spallation phenomenon in an arc-jet environment," Journal of Thermophysics and Heat Transfer, Vol. 29, No. 4, October 2015.

● General

- Written in C++
- Reads 3D Unstructured grid in CGNS format

● Parallelization

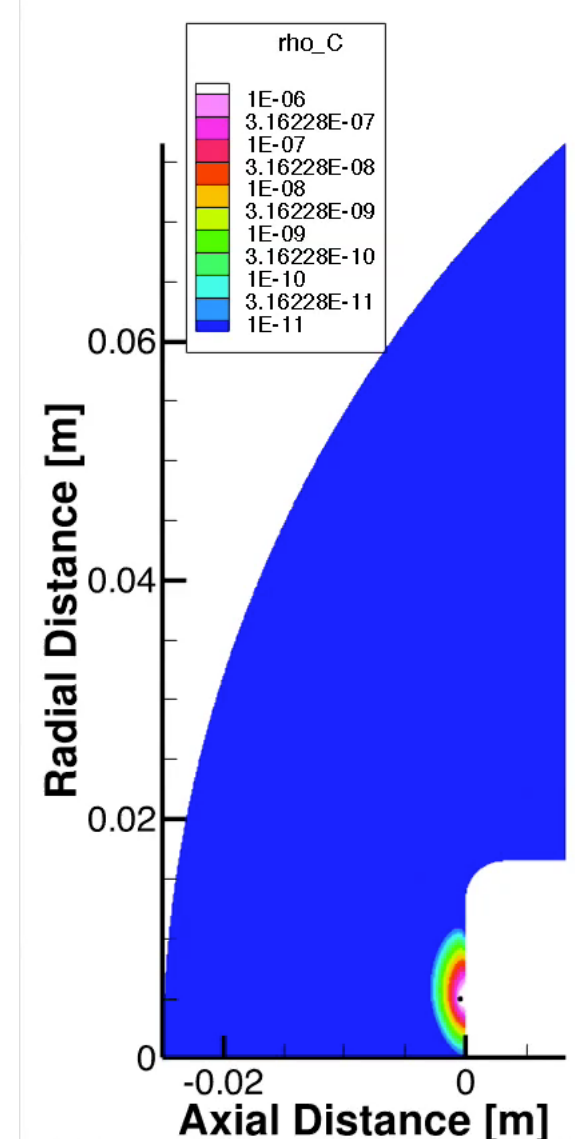
- ParMETIS for domain decomposition
- MPI for inter-processors communications
- PETSC Krylov subspace method as linear solver for iteration

● Spatial discretization

- Cell-centered finite volume method
- Second-order central differencing

● Time integration

- Fully implicit
- First-order backward Euler time integration
- Numerical flux Jacobian and analytical source Jacobian





KATS — Modeling Framework

- [1] Weng, H. and Martin, A., "Multidimensional modeling of pyrolysis gas transport inside charring ablative materials," Journal of Thermophysics and Heat Transfer, Vol. 28, No. 4, October–December 2014, pp. 583–597.
- [2] Weng, H., Bailey, S. C. C., and Martin, A., "Numerical study of iso-Q sample geometric effects on charring ablative materials," International Journal of Heat and Mass Transfer, Vol. 80, January 2015, pp. 570–596.
- [3] Weng, H. and Martin, A., "Numerical Investigation of Thermal Response Using Orthotropic Charring Ablative Material," Journal of Thermophysics and Heat Transfer, Vol. 29, No. 3, July 2015, pp. 429–438.
- [4] Davuluri, R. S. C., Zhang, H., and Martin, A., "Numerical study of spallation phenomenon in an arc-jet environment," Journal of Thermophysics and Heat Transfer, Vol. 29, No. 4, October 2015.

- 3D Conservation equations

$$\frac{\partial \mathbf{Q}}{\partial t} + \nabla \cdot (\mathbf{F} - \mathbf{F}_d) = \mathbf{S}$$

- Weak form after integrating over a finite volume

$$\int_V \frac{\partial \mathbf{Q}}{\partial t} dV = \int_V \nabla \cdot (\mathbf{F}_d - \mathbf{F}) dV + \int_V \mathbf{S} dV.$$

- Implicit backward Euler time integration, primitive variables introduced

$$\int_V \frac{\partial \mathbf{Q}}{\partial t} = \int_F (\mathbf{F}_d - \mathbf{F}) \cdot \mathbf{n} + \int_V \mathbf{S}$$

- Apply Gauss theorem

$$V_{cl} \frac{\partial \mathbf{Q}}{\partial t} = \sum_{face} (\mathbf{F}_d - \mathbf{F})_j \cdot \mathbf{n}_j A_j + \mathbf{S} V_{cl} \equiv \mathbf{R}^{n+1} = \mathbf{R}^n + \frac{\partial \mathbf{R}^n}{\partial \mathbf{P}} \Delta \mathbf{P}$$

- Primitive variables formulation

$$\left[\frac{V}{\Delta t} \frac{\partial \mathbf{Q}}{\partial \mathbf{P}} - \frac{\partial \mathbf{R}}{\partial \mathbf{P}} \right] \Delta \mathbf{P} = \mathbf{R},$$



KATS - Fluid Dynamics

$$\frac{\partial \mathbf{Q}}{\partial t} + \nabla \cdot (\mathbf{F} - \mathbf{F}_d) = \mathbf{S}$$

$$\mathbf{Q} = \begin{pmatrix} \rho_1 \\ \dots \\ \rho_{ns} \\ \rho u \\ \rho v \\ \rho w \\ E \\ E_{ve} \end{pmatrix}, \quad \mathbf{P} = \begin{pmatrix} \rho_1 \\ \dots \\ \rho_{ns} \\ u \\ v \\ w \\ T_{tr} \\ T_{ve} \end{pmatrix}, \quad \text{and} \quad \mathbf{S} = \begin{pmatrix} \dot{w}_1 \\ \dots \\ \dot{w}_{ns} \\ 0 \\ 0 \\ 0 \\ 0 \\ \dot{w}_v \end{pmatrix}$$

Mass flux

$$\mathcal{F} = \begin{pmatrix} \rho_1 u & \rho_1 v & \rho_1 w \\ \dots & \dots & \dots \\ \rho_{ns} u & \rho_{ns} v & \rho_{ns} w \\ \rho u^2 + p & \rho v u & \rho w u \\ \rho u v & \rho v^2 + p & \rho w v \\ \rho u w & \rho v w & \rho w^2 + p \\ (E + p) u & (E + p) v & (E + p) w \\ E_{ve} u & E_{ve} v & E_{ve} w \end{pmatrix}, \quad \mathcal{F}_d = \begin{pmatrix} -J_{x,1} & -J_{y,1} & -J_{z,1} \\ \dots & \dots & \dots \\ -J_{x,ns} & -J_{y,ns} & -J_{z,ns} \\ \tau_{xx} & \tau_{yx} & \tau_{zx} \\ \tau_{xy} & \tau_{yy} & \tau_{zy} \\ \tau_{zx} & \tau_{zy} & \tau_{zz} \\ \boldsymbol{\tau} \mathbf{u} - (\mathbf{q}_{tr} + \mathbf{q}_{ve}) - \sum_{i=1}^{ns} (\mathbf{J}_i h_i) \\ -q_{ve,x} - \sum_{i=1}^{ns} (J_{x,s} e_{ve,s}) & -q_{ve,y} - \sum_{i=1}^{ns} (J_{y,s} e_{ve,s}) & -q_{ve,z} - \sum_{i=1}^{ns} (J_{z,s} e_{ve,s}) \end{pmatrix}$$

Momentum fluxes

Convective fluxes

Diffusive fluxes

Energy flux

LeMANS

Le Michigan Aerothermodynamic Navier-Stokes Solver

- Governing equations

$$\frac{\partial \mathbf{U}}{\partial t} + \nabla \cdot (\mathbf{F} - \mathbf{F}_d) = \mathbf{C}$$

$$\mathbf{U} = \begin{pmatrix} \rho_1 \\ \vdots \\ \rho_{ns} \\ \rho u_x \\ \rho u_y \\ \rho u_z \\ E \\ E_{ve} \\ E_r \end{pmatrix} \quad \mathbf{F} = \begin{pmatrix} \rho_1 u_x & \rho_1 u_y & \rho_1 u_z \\ \vdots & \vdots & \vdots \\ \rho_{ns} u_x & \rho_{ns} u_x & \rho_{ns} u_x \\ \rho u_x^2 + p & \rho u_y u_x & \rho u_z u_x \\ \rho u_x u_y & \rho u_y^2 + p & \rho u_z u_y \\ \rho u_x u_z & \rho u_y u_z & \rho u_z^2 + p \\ (E + p)u_x & (E + p)u_y & (E + p)u_z \\ E_{ve} u_x & E_{ve} u_y & E_{ve} u_z \\ E_r u_x & E_r u_y & E_r u_z \end{pmatrix} \quad \mathbf{F}_d = \begin{pmatrix} -J_{x,1} & -J_{y,1} & -J_{z,1} \\ \vdots & \vdots & \vdots \\ -J_{x,ns} & -J_{y,ns} & -J_{z,ns} \\ \tau_{xx} & \tau_{xy} & \tau_{xz} \\ \tau_{yx} & \tau_{yy} & \tau_{yz} \\ \tau_{zx} & \tau_{zy} & \tau_{zz} \\ \mathbf{u}\boldsymbol{\tau} - (\mathbf{q}_t + \mathbf{q}_r + \mathbf{q}_{ve}) - (\mathbf{h}^T \mathbf{J}) \\ -\mathbf{q}_{ve} - (\mathbf{e}_{ve}^T \mathbf{J}) \\ -\mathbf{q}_r - (\mathbf{e}_r^T \mathbf{J}) \end{pmatrix} \quad \mathbf{C} = \begin{pmatrix} \dot{w}_1 \\ \vdots \\ \dot{w}_{ns} \\ 0 \\ 0 \\ 0 \\ 0 \\ \dot{w}_v \\ \dot{w}_r \end{pmatrix}$$

or, in vector form:

$$\frac{\partial}{\partial t} \begin{pmatrix} \boldsymbol{\rho} \\ \boldsymbol{\rho} \mathbf{u}^T \\ E \\ E_{ve} \\ E_r \end{pmatrix} + \nabla \cdot \left[\begin{pmatrix} \boldsymbol{\rho} \mathbf{u} \\ \boldsymbol{\rho} \mathbf{u}^T \mathbf{u} + I_p \\ (E + p) \mathbf{u} \\ E_{ve} \mathbf{u} \\ E_r \mathbf{u} \end{pmatrix} - \begin{pmatrix} -\mathbf{J} \\ \boldsymbol{\tau} \\ \mathbf{u}\boldsymbol{\tau} - (\mathbf{q}_t + \mathbf{q}_r + \mathbf{q}_{ve}) - (\mathbf{h}^T \mathbf{J}) \\ -\mathbf{q}_{ve} - (\mathbf{e}_{ve}^T \mathbf{J}) \\ -\mathbf{q}_r - (\mathbf{e}_r^T \mathbf{J}) \end{pmatrix} \right] = \begin{pmatrix} \dot{\mathbf{w}} \\ 0 \\ 0 \\ \dot{w}_v \\ \dot{w}_r \end{pmatrix}$$

3.3.2 Molecular Transport Processes

The molecular transport processes (diffusion, shear stress, thermal conductivity) affect all of the conservation equations. In this section, we study the evaluation of these terms for reacting air.

3.3.2 Molecular Transport Processes

a) Diffusion

Mass flux of species s into species t due to concentration gradient of species s is given by Fick's Law.

$$\Gamma_s = c_s(\mathbf{v} - \mathbf{v}_s) = -D_{st}\nabla c_s \quad (3.30)$$

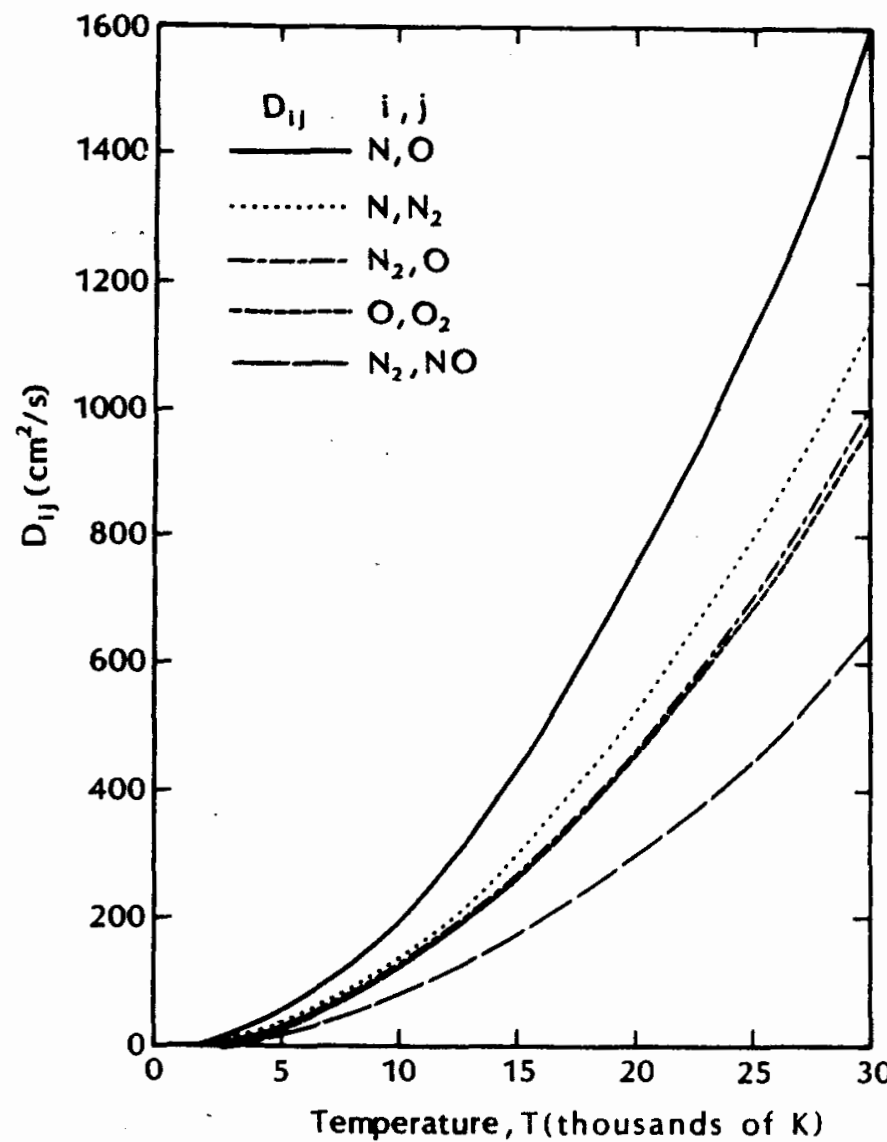
where

- ▶ D_{st} = diffusion coefficient, $\propto \langle c'_s \rangle \lambda$ from kinetic theory (3.31)
- ▶ $\langle c'_s \rangle$ = mean thermal speed of species $\propto \left(\frac{T}{m_s}\right)^{1/2}$
- ▶ λ = mean free path; $\frac{1}{\sqrt{2} n \sigma}$

Thus, D_{st} depends both on T and n . Examples of for air species are shown in the next figure. Diffusion can be omitted for non-reacting air.

3.3.2 Molecular Transport Processes

Diffusion



3.3.2 Molecular Transport Processes

Diffusion

Constant Lewis number (equal diffusion coefficients)

$$D = \frac{Le\kappa}{\rho C_p}$$

Binary diffusion coefficients

$$D_{sr} = \frac{k_{B,SI} T_{tr}}{p \Delta_{sr}^{(1)}(T_{tr})}$$

$$D_s = \frac{\gamma_t^2 M_s (1 - M_s \gamma_s)}{\sum_{r \neq s} (\gamma_r / D_{sr})}$$

3.3.2 Molecular Transport Processes

b) Viscosity

Shear stress for a Newtonian fluid:

$$\tau = \tau_{ij} = \mu \frac{du_i}{dx_j} \quad (3.32)$$

where μ = coefficient of viscosity

From tensor calculus:

$$\nabla \cdot \tau = \frac{\partial}{\partial x_j} \left[\mu \left(\frac{\partial u_i}{\partial x_j} + \frac{\partial u_j}{\partial x_i} \right) - \frac{2}{3} \mu \frac{\partial u_k}{\partial x_k} \delta_{ij} \right] \quad (3.33)$$

where the Kronecker delta is

$$\delta_{ij} = \begin{cases} 1 & i = j \\ 0 & i \neq j \end{cases}$$

Kinetic theory shows: $\mu \propto \rho \lambda \rightarrow \mu$ independent of density

3.3.2 Molecular Transport Processes

For non-reacting air, use Sutherland's Law:

$$\mu = 1.458 \times 10^{-6} \frac{T^{1.5}}{T + 110.4} \text{ kg/m-s} \quad (3.34)$$

For reacting air, situation is more complicated because chemical composition depends on T and p . The next figure shows ratio of actual μ to μ from (3.34). Major differences occur at high- T , for all p .

Note: μ also appears in Reynold's number:

$$\text{Re} = \frac{\rho u L}{\mu}$$

which is used to identify boundary layer behavior.

3.3.2 Molecular Transport Processes

Viscosity

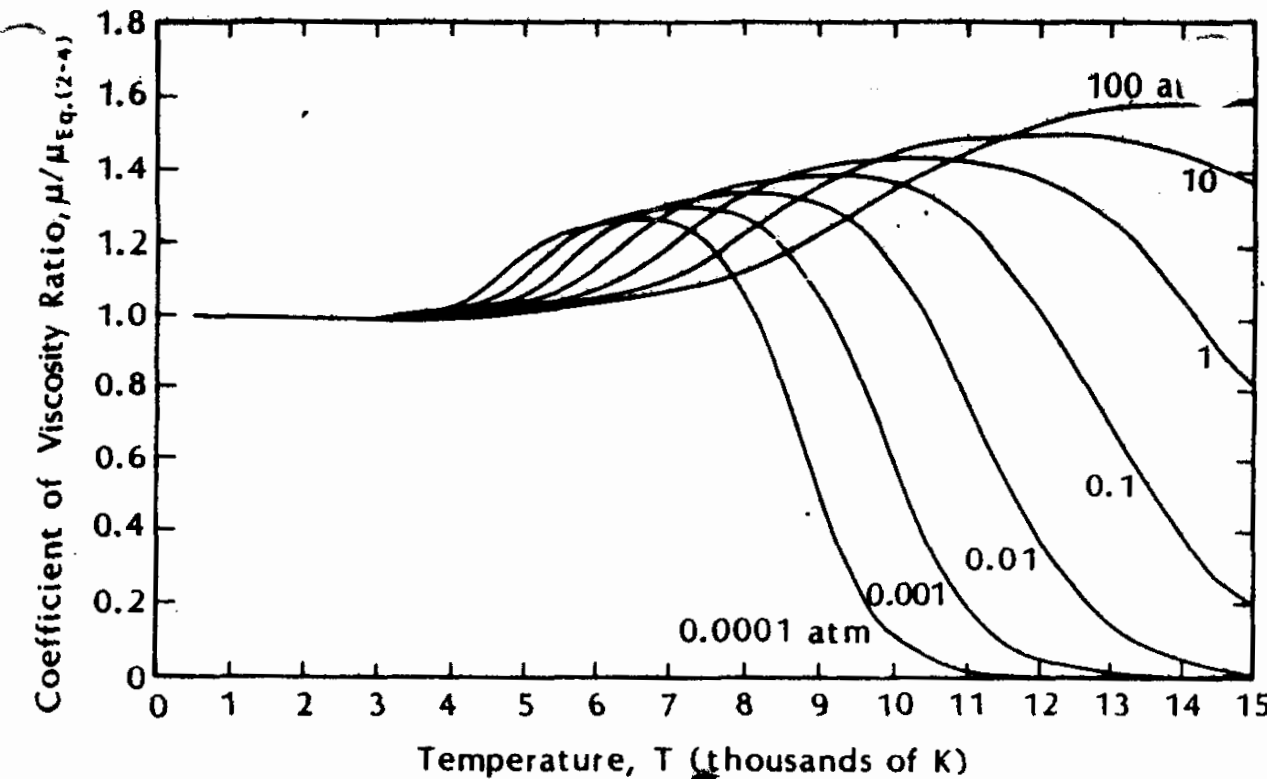


Fig. 2.4 Ratio of the coefficient of viscosity for air to the reference coefficient, Eq. (2-4), as a function of temperature, as taken from Ref. 11.

$$\mu_{eq} = 1.458 \times 10^{-6} \frac{T^{1.5}}{T + 110.4} \text{ kg/m-s} \quad (3.34)$$

3.3.2 Molecular Transport Processes

Mixing rule

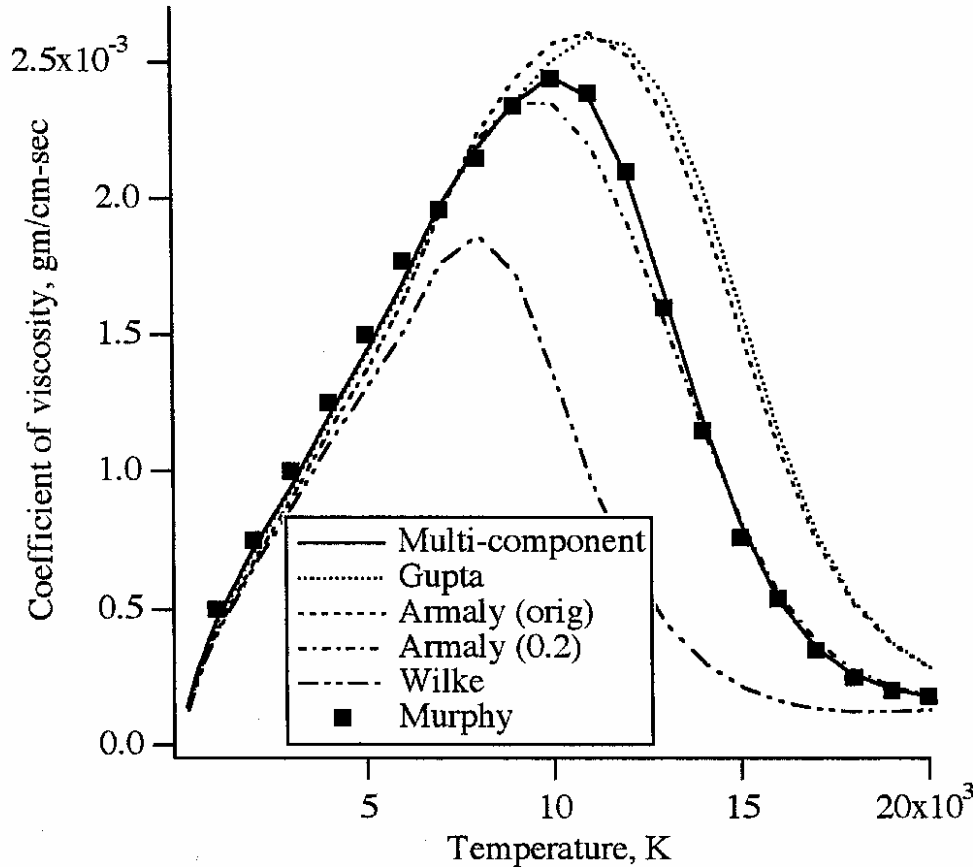


Fig. 1 Mixture viscosity for equilibrium 11-species air at 100 kPa.

Wilke

$$\eta = \sum_{j=1}^{NS} \frac{x_j \eta_j}{\phi_j}$$

$$\phi_i = \sum_{k=1}^{NS} \left[1 + \sqrt{\frac{n_i}{\eta_k}} \left(\frac{M_k}{M_i} \right)^{\frac{1}{4}} \right]^2 \Big/ \sqrt{8 \left(1 + \frac{M_i}{M_k} \right)}$$

Armaly-Sutton

$$\eta = \sum_{j=1}^{NS} \frac{x_j \eta_j}{\phi_j}$$

$$\phi_i = x_i + \sum_{k \neq i} x_k \left[\frac{5}{3} \frac{1}{A_{ik}^2} + \frac{M_k}{M_i} \right] \Big/ \left[1 + \frac{M_k}{M_i} \right]$$

$$= \sum_{i=1}^{NS} \left(x_i \Big/ \sum_{k=1}^{NS} \frac{x_k}{M_i} \frac{16}{5} \pi \sigma^2 \Omega_{ik}^{(2,2)*} \sqrt{\frac{2\mu_{ik}}{\pi k_b T}} \right)$$

$$\times \left[F_{ik} + B_{ik} \sqrt{\frac{n_i}{\eta_k}} \left(\frac{M_k}{M_i} \right)^{\frac{1}{4}} \right]^2 \Big/ \sqrt{8 \left(1 + \frac{M_i}{M_k} \right)}$$

Gupta-Yos

$$\eta = \sum_{i=1}^{NS} \left(x_i \Big/ \sum_{k=1}^{NS} \frac{x_k}{M_i} \Delta_{ik}^{(2)} \right)$$

$$= \sum_{i=1}^{NS} \left(x_i \Big/ \sum_{k=1}^{NS} \frac{x_k}{M_i} \frac{16}{5} \pi \sigma^2 \Omega_{ik}^{(2,2)*} \sqrt{\frac{2\mu_{ik}}{\pi k_b T}} \right)$$

Table 3 Relative computational cost of the methods used to compute mixture viscosity

Method	5-species air	11-species air	11 vs 5 species
Wilke ³	1.0	1.0	4.554
Armaly-Sutton ²	1.054	1.065	4.603
Gupta et al. ¹ -Yos ²⁴	0.891	0.919	4.697
Multicomponent (Gaussian)	1.927	2.098	4.958
Multicomponent (Cramer's rule)	1.979	2.250	5.177

If using numerical method, multi-component is even faster!

Computational cost of η

CG	1.00
Direct	1.51
Gupta-Yos	1.03
Wilke	2.16

[1] Palmer, G. E. and Wright, M. J., "Comparison of Methods to Compute High-Temperature Gas Viscosity," Journal of Thermophysics and Heat Transfer, Vol. 17, No. 2, April–June 2003.

[2] Magin, T. E. and Degrez, G., "Transport algorithms for partially ionized and unmagnetized plasmas," Journal of Computational Physics, Vol. 198, No. 2, 2004, pp. 424 – 449.

3.3.2 Molecular Transport Processes

c) Thermal Conductivity

Heat flux due to a temperature gradient is given by Fourier's Law:

$$\mathbf{q} = -\kappa \nabla T \quad (3.35)$$

where κ is the coefficient of thermal conductivity

Kinetic theory shows: $\kappa \propto \rho \lambda \rightarrow \kappa$ is independent of density

Sutherland's Law for non-reacting air:

$$\kappa = 1.993 \times 10^{-3} \frac{T^{1.5}}{T + 112} \frac{W}{m \cdot K} \quad (3.36)$$

3.3.2 Molecular Transport Processes

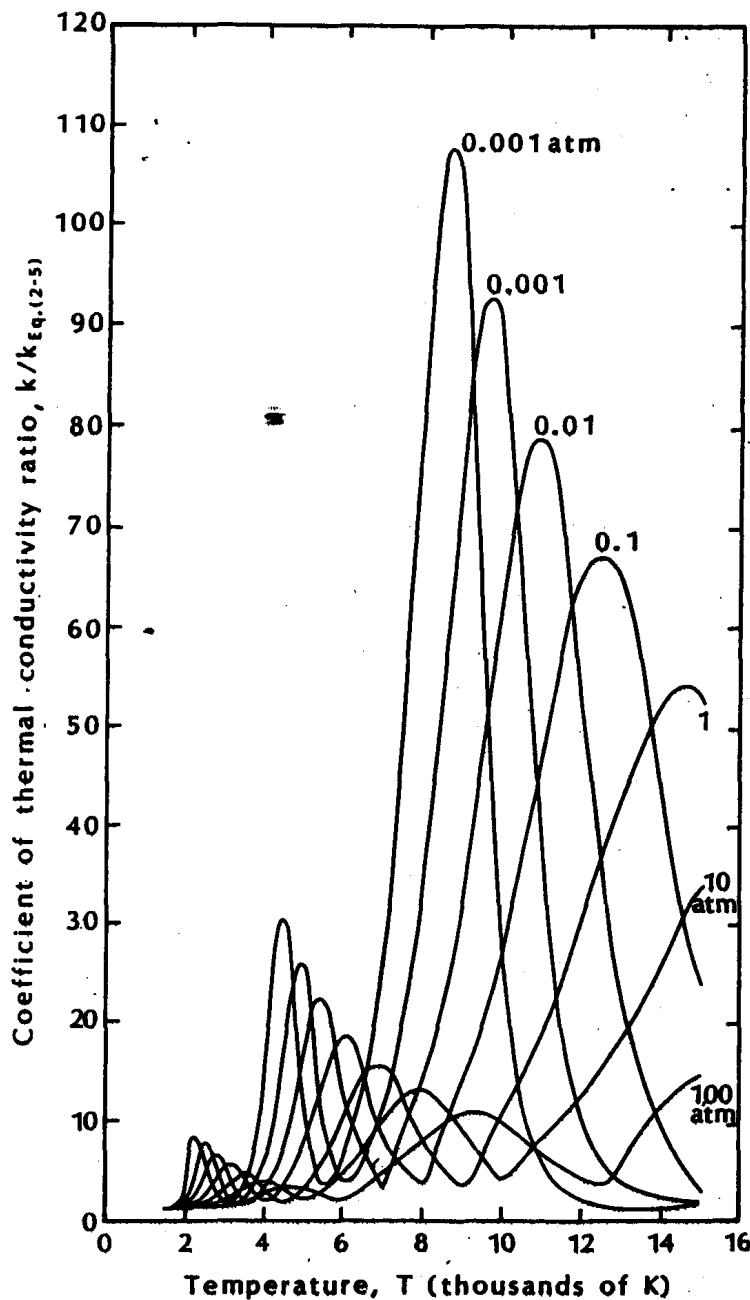
Viscosity and thermal conductivity can be linked using the Prandtl number, for non-reacting air:

$$\text{Pr} \equiv c_p \frac{\mu}{\kappa} \approx 0.75 \quad (3.37)$$

Thermal conductivity has even more complex dependance on T and p for reacting air. The next figure shows typical results with several maxima; these are due to:

- ▶ O₂ dissociation ($T \sim 3000$ K at $p = 1$ atm)
- ▶ N₂ dissociation ($T \sim 7000$ K at $p = 1$ atm)
- ▶ Atom ionization ($T \sim 14000$ K at $p = 1$ atm)

3.3.2 Molecular Transport Processes



Thermal conductivity

Fig. 2.6 Ratio of the coefficient of thermal conductivity of air to the reference coefficient, $k_{Eq.(2-5)}$, as a function of temperature, as taken from Ref. 11.

$$\kappa_{eq} = 1.993 \times 10^{-3} \frac{T^{1.5}}{T + 112} \text{ W/m-K} \quad (3.36)$$

3.3.2 Molecular Transport Processes

Thermal conductivity

Eucken's Law (with Wilke)

$$k_{tr,s} = \frac{5}{2}\mu_s Cv_{t,s} + \mu_s Cv_{r,s} \quad \text{and} \quad k_{ve,s} = \mu_s Cv_{ve,s}$$

$$\kappa = \sum_s^{ns} \frac{X_s \kappa_s}{\phi_s} \quad \phi_s = \sum_r^{ns} X_r \frac{\left[1 + \sqrt{\frac{\mu_s}{\mu_r}} \left(\frac{M_r}{M_s}\right)^{1/4}\right]^2}{\sqrt{8 \left(1 + \frac{M_s}{M_r}\right)}}$$

Gupta-Yos

$$\kappa_t = \frac{15}{4} k_{B,SI} \sum_{s \neq e} \frac{\gamma_s}{\sum_{r \neq e} a_{sr} \gamma_r \Delta_{sr}^{(2)}(T_{tr}) + 3.54 \gamma_e \Delta_{se}^{(2)}(T_{ve})}$$

$$\kappa_r = k_{B,SI} \sum_{s=mol} \frac{\gamma_s}{\sum_{r \neq e} \gamma_r \Delta_{sr}^{(1)}(T_{tr}) + \gamma_e \Delta_{se}^{(1)}(T_{te})}$$

$$\kappa_{vel} = k_{B,SI} \frac{Cv_{ve}}{R} \sum_{s=mol} \frac{\gamma_s}{\sum_{r \neq e} \gamma_r \Delta_{sr}^{(1)}(T_{tr}) + \gamma_e \Delta_{se}^{(1)}(T_{te})}$$

3.3.2 Molecular Transport Processes

Example 3.2

Calculate coefficients of viscosity, thermal conductivity and Prandlt number upstream and downstream the normal shock wave generated by the Shuttle at 70 km altitude in Earth's atmosphere assuming:

- a) Calorically perfect gas
- b) Real gas

3.3.3 Effects of transport

Navier-Stokes Eqns. for 1-D, steady-state non-reacting flow:

► mass:

$$\frac{d}{dx} \rho u = 0$$

► momentum:

$$\frac{d}{dx} \rho u^2 = -\frac{dp}{dx} + \frac{d\tau}{dx}$$

► energy:

$$\frac{d}{dx} \rho u \left(h + \frac{1}{2} u^2 \right) = \frac{d}{dx} (\tau v - q)$$

3.3.3 Effects of transport

Integration from region I upstream of shock, to a general point ($\tau_1, q_1 = 0$):

- ▶ mass: $\rho u = \text{const}$
- ▶ momentum: $\rho u^2 - \rho_1 u_1^2 = -(p - p_1) + \tau$
- ▶ energy: $\rho u(h + \frac{1}{2}u^2) - \rho_1 u_1(h_1 + \frac{1}{2}u_1^2) = (\tau v - q)$

3.3.3 Effects of transport

Thus:

- ▶ $\tau = q = 0$ give the normal shock jump conditions
- ▶ Finite τ, q give structure to normal shock

